Title

Diffusion of Protein Molecules through Microporous Nanofibrous Polyacrylonitrile Membranes

Journal

ACS Applied Polymer Materials, 3(3)

ISSN

2637-6105

Authors

Zhao, Cunyi
Si, Yang
Zhu, Shenghan
et al.

Publication Date

2021-03-12

DOI

10.1021/acsapm.0c01394

Peer reviewed

HHS Public Access

Author manuscript

ACS Appl Polym Mater. Author manuscript; available in PMC 2022 March 12.

Published in final edited form as:

ACS Appl Polym Mater. 2021 March 12; 3(3): 1618–1627. doi:10.1021/acsapm.0c01394.

Diffusion of Protein Molecules through Microporous Nanofibrous Polyacrylonitrile Membranes

Cunyi Zhao[1], **Yang Si**[1,#], **Shenghan Zhu**[1], **Kevin Bradley**[1], **Ameer Y Taha**[2], **Tingrui Pan**[3], **Gang Sun**[1,*]

[1]Department of Biological and Agricultural Engineering, University of California, Davis, CA 95616, USA.

[2]Department of Food Science and Technology, University of California, Davis, CA 95616, USA

[3]Department of Biomedical Engineering, University of California, Davis, CA 95616, USA

Abstract

Porous nanofibrous membranes have ultrahigh specific surface areas and could be broadly employed in protein purification, enzyme immobilization, and biosensors with enhanced selectivity, sensitivity, and efficiency. However, large biomolecules, such as proteins, have hindered diffusion behavior in the micro-porous media, significantly reducing the benefits provided by the nanofibrous membranes. The study of protein diffusion in polyacrylonitrile (PAN) nanofibrous membranes produced under varied humidity and polymer concentration of electrospinning revealed that heterogeneous structures of the nanofibrous membranes possess much smaller effective pore sizes than the measured pore sizes, which significantly affects the diffusion of large molecules through the system though sizes of proteins and pH conditions also have great impacts. Only when the measured membrane pore size is at least 1000 times higher than the protein size, the diffusion behavior of the protein is predictable in the system. The results provide insights into the design and applications of proper nanofibrous materials for improved applications in protein purification and immobilizations.

Keywords

Protein diffusion; Nanofibrous membrane; Micro-porous structure; Protein-polymer interaction; effective pore size; diffusion coefficient; partition coefficient

1. Introduction

Electrospun nanofibrous membranes possess ultrahigh specific surface areas and have become promising materials in air filtration, chemical separation, and protein purification.[1–4] The membranes have found increased applications in sensors, enzyme immobilizations, drug delivery, and protein separations.[5–7] Because of the ultrahigh specific

*Corresponding author: gysun@ucdavis.edu; Fax: +530-752-7584; Tel: +530-752-0840.
#Current address: College of Textiles, Donghua University, Shanghai, China

Supporting Information:
Additional research results are provided as supporting information.

surface areas, the nanofibrous membranes could immobilize enormous amounts of proteins on surfaces of nanofibers by either physical adsorption or chemical covalent bonding. Theoretically, the surface areas of the nanofibers could be hundreds or thousands of times higher than that of macro-sized fibrous materials, and the expected performance of the nanofibrous membranes should be increased accordingly. However, experimental results on the membranes were lower than the theoretically speculated values.[8–10] After analyzing the structural features of the nanofibrous membranes, inhibited diffusion of large biomolecules in the micro-porous nanofibrous membrane is considered to be caused by several factors.[11, 12] When large biomolecules flow through the porous materials, the diffusion of the molecules could be significantly decreased due to potential steric inhibition and solute-to-polymer interactions.[13–16] As a result, the number of loaded proteins inside the membranes could be lower than the theoretically expected values.

The diffusion of solutes in polymer network membranes was studied by assuming cylinder pore structures in the materials, and the influence of material structural properties on the diffusion of solutes was revealed[17]. Then, the impact of polymer properties, such as hydrophilicity and swelling ratios, on the diffusion of solutes in hydrogels was investigated[18,19] However, the hypothesized cylindrical pore structure may not fit the structural features of the electrospun microporous nanofibrous membranes, where randomly distributed pores exist in differently stacked layers of horizontal fiber webs. A hindered diffusion of spherical molecules through fibrous materials was investigated, and a correlation between fiber volume fraction and the diffusion coefficient was established.[20] Furthermore, the performance of the fibrous matrix in solute sieving was optimized by comparing the transport of spherical particles through the fibrous media and a row of parallel cylinders.[21] These results explained well on diffusions of inert molecules through fenestrated systems having weak interactions with the open and homogenous fibrous matrices. The diffusion of proteins in varied hydrogels or polymer solutions revealed the influence of matrix structures on diffusion coefficiency.[22–25]

The microstructures of the nanofibrous membranes are dramatically different from these polymeric materials. The hydrogels and polymer solutions are homogenous systems in three dimensions (3D), but the electrospun nanofibrous membranes are structures formed with a layer-by-layer accumulation of randomly oriented horizontal nanofiber webs. The pores in the top layer of the fibrous webs could be blocked by another layer of similar webs underneath,[26–28] leading to the fact that the measured pore size of a membrane could be significantly larger than the pore size that a molecule diffusing through the membrane will encounter. Here, we define this pore size of the membrane as the effective pore size of the membrane, which could be significantly smaller than the measured pore sizes of membranes. This is a special structural feature of the nanofibrous membranes, which has not been addressed in the literature.

The special structural feature could affect the transport of large molecules such as proteins through the vertical direction of the nanofibrous membranes. Such a feature makes the nanofibrous membranes excellent filter media for ultrafiltration,[29] but potentially reducing the loading of enzyme molecules to surfaces of nanofibers inside the membranes and consequently lowering desired sensitivity of the biosensors. Meanwhile, the ultrahigh

specific surface areas of the nanofibrous materials could enhance interactions with biomolecules during the diffusion process. Thus, the transport behavior of larger biomolecules through the system should be investigated systematically.

In this work, microporous nanofibrous membranes were prepared by electrospinning a diluted polyacrylonitrile (PAN) solution and employed to investigate the diffusion of proteins through the fibrous media. The PAN membranes are structurally stable in aqueous systems. The membrane morphologies were controlled with varied sizes of fiber diameter and membrane pore prepared by adjusting electrospinning conditions. A side-by-side diffusion chamber was used to measure diffusion coefficients of proteins in the fibrous membranes with varied porosity and fiber diameters, which also simulate the loading of biomolecules on the membranes during the preparation of biosensors.[5] The diffusions of proteins in this system were affected by a size ratio between protein and measured pores, protein-polymer interactions, and properties of proteins employed in diffusion studies. Diffusions of proteins in the nanofibrous membranes were analyzed using theoretical models applied for 3-dimensionally homogenous polymer systems. The results revealed that only the membrane with very large pores could match the modeled diffusion behavior of large molecules and the heterogeneous structures of the membranes in the diffusion direction significantly reduced the diffusion of large molecules inside the nanofibrous membrane materials.

2.1 Materials and method

2.1. Materials.

Polyacrylonitrile (PAN, M_n=150,000), bovine serum albumin (BSA), lysozyme, human immunoglobulin G (IgG), and horseradish peroxidase (HRP) were obtained from Sigma-Aldrich (USA). N, N-Dimethylformamide (DMF), phosphate-buffered saline (PBS pH=7.4) citrate buffer (pH=4.4), sodium bicarbonate ($NaHCO_3$), and sodium carbonate (Na_2CO_3) were supplied by Fischer Scientific (USA). Pierce™ BCA protein assay kit was purchased from Thermo Fisher Scientific (USA).

2.2 Fabrication of fibrous membranes

PAN was dissolved in DMF at 80 °C to prepare varied concentrations of PAN in 6, 7, 8, 10, 12 wt. %, respectively. Then, the PAN solutions were transferred into 20mL syringes and loaded on infusion single-channel syringe pumps (Kats Scientific Co.). A 6/G needle was caped on a syringe, and the feeding rate was set at 2 mL/hr. A high voltage of 20 kV was employed on the needle tip, generating a continuous jet stream. The relevant PAN nanofibers were deposited on an aluminum foil-covered rotating receiver with a fixed distance of 20 cm. In controlling pore sizes of the membranes, the humidity of the electrospinning chamber was adjusted to 30%, 40%, 50%, 60%, and 70% relative humidity, respectively, by using a humidifier (Urpower Co.). The temperature was controlled at 25 ±1 °C for all PAN solution. Residual DMF solvent was removed by drying the produced PAN nanofibrous membranes in a vacuum oven at 80 °C for 2 hours.

2.3 Characterization of fibrous membranes

Morphologies of the PAN nanofibrous membranes were obtained by a scanning electron microscope (SEM, Quattro ESEM, Thermo Scientific™). The pore size and the distribution of fiber sizes of the membranes were measured with a capillary flow porometer (Porous Media Inc., Ithaca, NY). Fiber diameter was measured from SEM images with the help of a photoshop program. The thickness of the PAN membranes was measured through an electronic micrometer thickness gauge (Neoteck). The fiber volume fraction and porosity of the membranes could be calculated by the mass, apparent volume and density of PAN polymer.

2.4 Measurement of protein diffusion in fibrous membranes

Protein diffusion in the fibrous membrane was measured by using a side-by-side diffusion chamber (PerneGear Co.) which consists of two 3.4 mL chambers with a 9mm orifice. A PAN fibrous membrane was mounted between two chambers, and chambers were well sealed and placed in a water bath to maintain the temperature at 25 °C. Then, 3 mL of a PBS solution was added to each chamber respectively for prewetting the membranes. After 2 hours, 0.3 mL of a protein solution (10g/L in PBS buffer) was injected into the donor chamber, while the same amount of the PBS solution was added into the receptor chamber at the same time. Stirring bars were placed in both chambers and maintained at 750 rpm rate during the experiments. 20 μL of the sample solution was taken from each chamber at regular intervals and replaced with the same amount of the PBS buffer solution for at least 5 hours; then, the samples were diluted with 80 μL of the PBS buffer. The protein concentration was measured with the Pierce BCA protein assay kit (Thermo Fisher™). The working agent was prepared by mixing 50-parts Bicinchoninic acid (BCA) reagent A with 1-part Cu_2SO_4 reagent B. 100 μL of diluted protein sample was added into a test tube, mixing with 2 mL of the working agent, and the test tube was placed in a 37 °C oven for 30 mins. Protein concentration can be obtained with a UV-vis spectrophotometer (Thermo Scientific™) by calibration curves, as shown in supplement information (Figure S1). Then, the protein concentration in the receptor chamber at increment time could be used to quantitatively determine protein diffusion property inside membranes.

2.5 Measurement of loaded protein ratio in fibrous membranes

Loaded protein ratio is defined as the ratio of protein concentration in a membrane to protein concentration in a solution at the equilibrium of protein adsorption and desorption. Protein concentration in the membrane can be obtained by the amount of protein in the membrane divided by the volume of the membrane. For measuring protein amount in a membrane, the PAN membrane was removed from the chambers and dried in a vacuum oven for 10 mins after the diffusion experiment. Then, the membrane was placed in 10mL working agents following the BCA process, and the concentration of the protein desorbed from the membranes was measured. The fibrous membrane volume was obtained by the measured membrane area and thickness. Meanwhile, protein concentration in a solution can be obtained by measuring protein concentration in both donor and acceptor chamber after the diffusion experiment.

3. Results and Discussion

3.1 Fabrication of PAN nanofibrous membranes

The fiber diameters of the prepared fibrous membranes were varied from tens of nanometers to sub-micrometers, while the pore sizes were in micrometer scales. The influence of the membrane morphology on protein diffusion can be described in Scheme 1. Firstly, proteins can be blocked by the porous fibrous matrices if the protein sizes are close to the average pore sizes (Scheme 1a), but the membranes containing large pore exhibits less hindrance to protein molecules to pass through (Scheme 1b). Secondly, when a protein molecule passes through a pore, its motion may be hindered by the interactions between the protein molecules and surfaces of the fibers and hydrodynamic drag (Scheme 1c). Thus, the morphology of the membrane exhibits a significant influence on protein diffusion.

The PAN nanofibrous membranes in different morphologies were fabricated by adjusting two parameters during electrospinning, polymer concentration and relative humidity. The SEM images of the corresponding nanofibrous membranes are shown in Figure 1a. All the membranes revealed layered microporous fibrous structures with fibers randomly distributed horizontally and gradually reduced pore sizes from top to inside through the membranes. The fiber diameters and measured pore sizes show significant differences among these membranes, affected by the polymer concentration and relative humidity during the electrospinning (Figure 1b, 1c and 1d). The fiber diameter increased almost linearly to the increase of polymer concentration in spinning solutions (Figure 1b). As shown in Figure 1c–d, the measured pore size distributions ranged from 0.19 to 3.4 μm, and the measured pore sizes gradually increased from the membranes produced in polymer solutions of 6–12 wt%. The measured maximum pore size and average pore size both followed the same increase tendency as fiber diameter increased. As relative humidity increased from 30% to 60%, the measured pore size distribution gradually increased from 0.9 to 3.8 μm, but the pore size dramatically jumped to 9 μm at 70% RH, even though the nanofiber diameter linearly increased as the relative humidity was raised (Figure 1e–g). These different nanofibrous membranes were employed in the following protein diffusion studies.

3.2 Derivation for protein diffusion in fibrous membranes

A side-by-side diffusion chamber was employed to measure protein transport in the PAN nanofibrous membranes (Figure 2a). Fick's Law was applied to calculate the diffusion of proteins in each membrane (Equation 1).[30, 31]

$$J = -D_{eff}\frac{dC}{dx} \quad (1)$$

Where J is diffusion flux, which can be converted to the change of protein amount in each chamber at the membrane boundary at each chamber side, D_{eff} is the effective diffusion coefficient of protein in membranes, C is protein concentration, and x is the diffusion distance.

The morphology and pore structure of the membranes were not affected by PBS buffer solutions, which were supported by the SEM images (Figures 2b and 2c). Thus, the protein

concentration in the membranes can be hypothesized as linearly decreasing from the donor chamber boundary to the receptor chamber boundary at a pseudo steady-state[32]. And the protein could be considered as diffusing in a consistent porous system.

The diffusion coefficient could be determined by the following equation at the pseudo steady-state (Equation 2)[32]:

$$\ln\left(1-\frac{2c_2}{c_0}\right)=-\frac{2D_{eff}k_dA}{V\Delta x} \quad (2)$$

Where C_0 and C_2 are the initial protein concentration in the donor chamber and protein concentration in the receptor chamber at a specific time. D_{eff} is the effective or apparent diffusion coefficient, and K_d is the partition coefficient of the protein. A is the protein diffusion area, V is the donor chamber volume, and Δx is the thickness of the membrane.

The effective diffusion coefficient could be calculated from a slope yielded by a plot of $\Delta x * \ln(1-2c_2/c_0)$ versus t with a known partition coefficient. As mentioned in the experimental section, the partition coefficient of a protein is defined as the ratio of protein concentration in the membrane (c_m) to protein concentration in solution (c_s), which can be obtained by measuring the amount of protein (Q_m) in membrane and protein concentration in the donor chambers (c_1) and receptor chamber (c_2), respectively (Equation 3).

$$k_d=\frac{c_m}{c_s}=\frac{Q_m/A\Delta x}{(c_1V+c_2V)/2V} \quad (3)$$

3.3 Diffusion of BSA in various nanofibrous membranes

The as-prepared nanofibrous membranes were employed to investigate the influence of pore structure and fiber diameter on the diffusion and partition coefficient of BSA (Figure 3). The morphology of the membranes has a significant influence on the adsorption of the protein on the surface of the nanofibers. As shown in Figure 3a, the partition coefficient of the protein on the membrane increased as the relative humidity (RH) in the electrospinning chamber increased from 30% to 50%, which are the same as the increment of fiber diameter and pore size (Figures 1e and 1g). Then, the partition coefficient decreased after RH reached 60% and dramatically reduced at 70% RH due to large pore size and reduced interactions of the protein with surfaces of the nanofibers. The same tendency of the partition coefficient was observed in the membranes prepared with different polymer concentrations (Figure 3b). The partition coefficient increased as the pore size increases from 6 wt % to 10 wt% of PAN and reached a peak at 10 wt% and slightly decreased at 12 wt% because of the oversized nanofiber diameter and reduced surface areas of the membranes (Figures 1b and 1d). Here, the loaded protein ratios per mass of membranes could better represent the amounts of the proteins adsorbed onto the membranes, which were obtained by taking the loaded protein ratios (c_m/c_s) divided by apparent densities of the membranes (d). The loaded protein ratios per mass of membrane increase with the increase of humidity and polymer concentration and reach peaks at proper parameters. The smaller nanofiber diameter represents a higher specific surface area and prompts more adsorption of the protein. Meanwhile, the amount of

the loaded protein onto the surfaces of the fibers is also limited by the measured pore size of the membranes because protein molecules cannot reach fiber surfaces inside the membranes efficiently in the small pore samples.

The plots of the cumulative amounts of the protein in the receptor chamber versus time are shown in Figure 3c and 3d. The amounts of the diffused protein revealed a significant difference among different membranes. A pseudo steady-state of diffusion of the protein could be maintained more than four hours in a membrane with smaller fiber diameter and pores, prepared under 30% RH, and a gentle slope in the linear range representing slow diffusion of the protein inside the membrane. However, it took almost 60 minutes to reach the pseudo steady-state during the diffusion process. Then, the time to reach pseudo steady-state diffusion dramatically reduced, and the slopes of curves became steeper with increased fiber diameter and pore sizes, controlled by increased relative humidity from 30%-70%. Especially, the diffusion of the protein through a membrane prepared under 70% RH could achieve pseudo steady-state in a very short time, representing the membrane has negligible hindrance to protein diffusion. Similarly, the pseudo steady-state diffusion of the protein through the membranes with varied fiber and smaller pore using different polymer concentrations duplicated the pattern. Overall, large measured pores dramatically reduced the times to reach pseudo steady-state diffusion in the membranes.

The diffusion of protein in all membranes could achieve the pseudo steady-state representing the concentration of protein inside pores should maintain constant. Although the concentration of the adsorbed protein may change at pseudo steady-state, this protein has no contribution to the diffusion. Thus, the effective diffusion coefficient could be calculated by Equation 2 with the slop in the linear range. The ratios between the effective diffusion coefficient to the bulk diffusion coefficient (D_{eff}/D_0), which could be obtained by the reference[33], are shown in Figures 3e and 3f. The trends of the changes are consistent with the measured pore sizes and fiber diameters (Figures 1b,1d,1e, and 1g). However, the increases of the diffusion coefficient of the membranes with the increases in humidity and polymer concentration all correlate to the increase of measured pore sizes in the membranes. The membranes with similar pore size but different fiber diameter (such as the membranes prepared under 50% RH and 10% wt) exhibited similar diffusion coefficients. Contrarily, the membranes with similar fiber diameters but different pore sizes (such as the membranes made under 70% RH and 12% wt) present significant differences. Overall, the protein diffusion coefficient increased as the measured pore size of the membranes was enlarged.

3.4 Modeled diffusion of protein through nanofibrous membranes

Both humidity and concentration of the polymer solution of electrospinning affected fiber diameter and pore size of the membranes. Here, we would like to assign two ratios (r_s/r_p, r_s/r_f) of the membranes to represent the relative ratios of average measured pore size (r_p) and fiber diameter (r_f) to the size of protein (r_s), respectively, which could be used to find the relationship to effective diffusion pattern of the protein. A correlation between the protein size (r_s) to the measured pore size (r_p) ratio (r_s/r_p) or the protein size(r_s) to fiber diameter (r_f) ratio(r_s/r_f) with diffusion coefficient ratios (D_{eff}/D_0) is shown in Figure 4. The diffusion coefficient ratios dramatically decreased when the r_s/r_p ratio increased from 0 to 0.002, then

reduced to hundreds of times lower as the r_s/r_p ratio further increased to 0.01. These results indicate that protein diffusion behaviors are different in nanofibrous membranes versus other polymer media. In general, the diffusion of proteins may be mainly affected by the steric hindrance and hydrodynamic interactions in a classical polymer network material, such as a hydrogel. And the protein adsorption on the polymeric media was negligibly considered in the literature.[18, 34, 35] Firstly, the D_{eff} inside a classical fibrous membrane would be similar to the D_0 when the r_s/r_p ratio is lower than 0.01.[24, 36, 37] But the diffusion coefficients inside the nanofibrous materials are significantly lower than diffusion coefficients in other classical systems, indicating that the strong adsorption of proteins on the surfaces or potential blockage of the protein by the nanofibrous membranes occurs here.[38–40] Since the physically adsorbed or blocked proteins have no contribution to the diffusion, the protein diffusing through pores and protein adsorbed onto the fiber need to be discriminated, which could be calculated by following Equation 4,

$$C = \varphi * n + (1 - \varphi) * C^L \tag{4}$$

Where C is the total protein concentration in the membrane, C^L is the concentration of non-adsorbed protein in the pores, n is the amount of adsorbed protein on fiber surfaces inside the membrane, and φ is the volume fraction of fiber inside the membranes. Then, the diffusion equation (Equation 2) could be extended to account for the adsorbed protein as distinct from the protein in the pores (Equation 5).

$$\frac{\partial C(t,x)}{\partial t} + \left(\frac{\varphi}{1-\varphi}\right)\frac{\partial n(t,x)}{\partial t} = D\frac{\partial^2 C^L(t,x)}{\partial x^2} \tag{5}$$

Where D is the solute diffusion coefficient through the pores. To calculate the diffusion coefficient, the kinetics of protein adsorption need to be described. Here, we impose a simplest approach by assuming local equilibrium with Henry's adsorption[41, 42], or Equation 6.

$$n = KC^L \tag{6}$$

Where K is Henry's adsorption constant of protein on fibers. The local equilibrium represents the protein adsorption is reversible and the rates of adsorption and desorption are faster than the rate of diffusion. Based on the literature, the kinetic adsorption constant of BSA on the PAN surface is at 10^{-4} cm/s,[43] but the diffusion constant of BSA in PBS buffer is at 10^{-7} cm^2/s range[44]. Meanwhile, D.E. Liu et al. also proved that the local equilibrium could be achieved when the solute-polymer interactions are modest.[18] Substitution of Equation 6 into Equation 5 yields the effective diffusion coefficient (D_{eff}) in Equation 7.

$$D_{eff} = \frac{D}{1 + \frac{\varphi}{1-\varphi}K} \tag{7}$$

Henry's adsorption constant is required to solve Equation 7. However, since the adsorption proceeds with diffusion simultaneously, the direct measurement of the kinetic adsorption

constant is complicated.[45–47] Here, we employed D.E. Liu's method: calculating adsorption constant by using the partition coefficient following Equation 8.[41, 42]

$$\frac{k_d}{1-\varphi} = E_{ex}E_{ad} \tag{8}$$

Where E_{ex} indicates a size-exclusion factor, or the volume of liquid available to the protein in the membrane divided by the total pore volume of membrane; and E_{ad} designates protein adsorption factors. For protein in a matrix with randomly oriented fibers, the E_{ex} could be presented by the classical Ogston equation (Equation 9).[48, 49]

$$E_{ex} = \exp[-\varphi\left(1+\frac{r_s}{r_f}\right)^2] \tag{9}$$

Where r_s and r_f indicate the diameters of protein and fiber, respectively. The pore size was measured by a capillary flow porometer, where the pores among the fibrous membranes are equivalent to the capillary pores. Thus, the size exclusion factor also could be represented by the solute in capillary pores (Equation 10).[50]

$$E_{ex} = \varphi(1-\frac{r_s}{r_p})^2 \tag{10}$$

Where r_p is the diameter of the measured pore sizes. Based on Equation 6, the E_{ad} could be represented by the Henry adsorption constant (Equation 11).

$$E_{ad} = \left(1+\frac{\varphi}{1-\varphi}K\right) \tag{11}$$

Thus, the kinetic adsorption constant could be solved by combining Equations 8–11. The adsorption constants (E_{ad}) of the membranes are about 40, indicating a strong interaction between protein and the fibrous matrix. (The fiber volume fractions and adsorption constants of each membrane are listed in Table S1 in supplementary information)

For a better understanding of the unique property of the transport of proteins inside the nanofibrous membrane, the experimental data were compared with the modelling results. Table 1 shows classical physical interaction-based diffusion theories that could predict the hindered diffusion of solutes in fibrous membranes. The effective diffusion coefficient (D_{eff}) of each model could be calculated via Equation 7 with obtained Henry's adsorption constants. The predicted results from each model overestimated the experimental results (represented as the line in Figure 4). The large discrepancy between measured effective diffusion coefficients and predicted results indicates the classical hindered diffusion theories are not fully suitable to the electrospun nanofibrous membranes. Different from the classical 3D homogenous fibrous membrane, the electrospun nanofibrous membranes are layer-by-layer assemblies and heterogeneous in the vertical direction from the planar areas. The SEM images of the top view and cross-section of the electrospun nanofibrous membrane indicate the different morphology between horizontal direction and vertical direction. (Figure S2 at supplementary information) Thus, the tortuosity of the nanofibrous membranes

is dramatically high, making the classical modelling unfit to the nanofibrous membranes. From the images, the measured pore sizes of every nanofibrous layer were blocked by the top and bottom layers of nanofibers, resulting in much smaller effective pores in the vertical direction of the nanofibrous membranes. Literature also showed that predicted pore sizes of multilayered nanofibrous membranes are reduced.[51, 52] Therefore, only very large pored nanofibrous membranes may still retain a real large effective pore size (r'_p) and small protein size (r_s) to pore size (r'_p) (r_s/r'_p) ratio. In fact, the effective diffusion coefficient of the membrane with the largest measured pore size (70%RH membrane) matched well with theoretical results, indicating the modelling analysis was meaningful but most nanofibrous membrane structures are not homogeneous in the diffusion direction and unfit for the model. Similar results were also obtained by measuring the diffusion coefficient of BSA in a nitrocellulose membrane in the literature.[53] The diffusion coefficient of BSA in that membrane is hundreds of times lower than the bulk diffusion coefficient even when the pore size is over 1 μm.

3.5 Influence of protein-polymer interaction on protein diffusion

Besides the morphology of the membranes, adsorption (partition) and diffusion of proteins in the systems are also affected by the chemical structures of fiber forming polymers. Generally speaking, the protein-polymer interactions consist of ionic force, hydrophobic force, dipole-dipole interactions, and hydrogen bonds. Among them, hydrogen bonds, hydrophobic and polar interactions are the dominating forces between proteins and PAN polymer because acrylonitrile unit has a highly polar nitrile group and a lone pair of electrons on the nitrogen, potentially forming hydrogen bonds with proteins and possessing negative charges on fiber surfaces in solutions. Such interactions can be adjusted by applying different pH buffers, as shown in Figure 5. Since BSA (isoelectric point=5.4) possesses more negative charges as pH values of the buffer solutions are above its isoelectric point, the diffusion of the protein was prompted due to increased repulsion between the protein and the nanofiber at pH values of 5.5–10.4. (bulk diffusion coefficient of BSA at varied pH buffer was obtained from ref[59]). The low diffusion coefficient ratio of BSA at pH = 5.4 was probably due to the low solubility of the protein close to the isoelectric point. Afterward, as the pH increases, the diffusion coefficient of the protein increased. But the increased repulsion reduced adsorption amounts of BSA on the fiber surfaces. Based on the above results, both the adsorption and diffusion of the protein in the fibrous membranes are highly determined by the protein-fiber interactions as well. The stronger protein-fiber repulsion prompts protein diffusion but sacrifices protein adsorption of the membranes.

3.6 Diffusion of different proteins in nanofibrous membranes

Considering actual applications of the nanofibrous membranes in protein separation and purification applications, protein properties, such as protein size and isoelectric point (pI), on their diffusion performances also were investigated. Four proteins were selected to study their corresponding protein diffusion performances. (Table 2) Since the concentration of each protein in the side-by-side chamber is low, protein molecules could be simplified as spherical particles diffusing in the nanofibrous membranes, and radiuses of the proteins were estimated based on literature data.[32,35,38,40] A nanofibrous membrane made from 10 wt% of

PAN DMF solution under 50% RH was selected in this study, and a PBS buffer served as the media.

Partition and diffusion coefficients of the proteins are shown in Figure 6. Lysozyme (pI=11.35) reveals the highest partition coefficients on the membrane among all proteins because it carries more positive charge at the PBS buffer and prompts the strongest protein-fiber attraction. The strong protein-fiber attraction hinders the diffusion of lysozyme in the nanofibrous membrane and provided the lowest diffusion coefficient even with the smallest size among all proteins. Immunoglobulin G (IgG) is a large size protein but has a similar loaded protein ratio as BSA. And it presents a lower diffusion coefficient in the membranes as speculated due to the large IgG protein size (5.4nm) hindering the diffusion. Horseradish peroxidase (HRP) contains more positive charge than BSA at the PBS buffer; thus, it has a higher partition coefficient but a similar diffusion coefficient as BSA.

4. Conclusion

The protein diffusion and partition coefficient, the two vital factors describing protein transport behavior in nanofibrous membranes, were investigated in this study, which is the first step to reveal the impact of nanofibrous membrane structures on diffusions of large biomolecules in the system. Different from classical solute diffusion models in a 3-D homogenous fibrous material, the electrospun nanofibrous membranes contain layered unparallel pores with large pore sizes in each layer, and the pores of each nanofiber layer are blocked by the top and bottom layers, resulting in smaller effective pore sizes in the membranes. The protein diffusion is profoundly affected by the membrane morphology and protein-polymer interactions. The effective pore size of the membranes has a dominating impact on both protein diffusion and adsorption. The polymer-protein interactions significantly affect protein adsorption on fiber surfaces, but the repulsive inter-molecule force could enhance protein diffusion through the membranes. Overall, the diffusion of protein and loaded protein ratios on membranes is determined by effective pore sizes of the membranes, protein sizes and buffer pH conditions in the media.

Supplementary Material

Refer to Web version on PubMed Central for supplementary material.

Acknowledgements:

This work was supported by the NIEHS superfund center (project # NIH 5P42ES004699) at University of California, Davis and a USDA-NIFA grant # 2018-67017-28116.

5. References

1. Sundarrajan S; Tan KL; Lim SH; Ramakrishna S, Electrospun nanofibers for air filtration applications. Procedia Eng. 2014, 75, 159–163.
2. Ge J; Zong D; Jin Q; Yu J; Ding B, Biomimetic and superwettable nanofibrous skins for highly efficient separation of oil-in-water emulsions. Adv. Funct. Mater2018, 28 (10), 1705051.
3. Zhu J; Sun G, Facile fabrication of hydrophilic nanofibrous membranes with an immobilized metal–chelate affinity complex for selective protein separation. ACS Appl. Mater. Interfaces2014, 6 (2), 925–932. [PubMed: 24377297]

4. Tang P; Zhang M; Ji B; Yong T; Sun G, Hierarchical Nucleophilic Nanofibrous Membranes for Fast, Durable, and Bare-Eye Visible Detoxification of Carcinogenic Alkylating Toxicants. Adv. Funct. Mater2019, 29 (50), 1905990.
5. Zhao C; Si Y; Pan B; Taha AY; Pan T; Sun G, Design and fabrication of a highly sensitive and naked-eye distinguishable colorimetric biosensor for chloramphenicol detection by using ELISA on nanofibrous membranes. Talanta2020, 121054. [PubMed: 32498843]
6. Zhu J; Sun G, Lipase immobilization on glutaraldehyde-activated nanofibrous membranes for improved enzyme stabilities and activities. React. Funct. Polym2012, 72 (11), 839–845.
7. Yu D-G; Zhu L-M; White K; Branford-White C, Electrospun nanofiber-based drug delivery systems. Health2009, 1 (02), 67.
8. Haider A; Haider S; Kang I-K, A comprehensive review summarizing the effect of electrospinning parameters and potential applications of nanofibers in biomedical and biotechnology. Arab. J. Chem2018, 11 (8), 1165–1188.
9. Rezaei B; Ghani M; Shoushtari AM; Rabiee M, Electrochemical biosensors based on nanofibres for cardiac biomarker detection: A comprehensive review. Biosens. Bioelectron2016, 78, 513–523. [PubMed: 26657595]
10. Fu Q; Duan C; Yan Z; Si Y; Liu L; Yu J; Ding B, Electrospun nanofibrous composite materials: a versatile platform for high efficiency protein adsorption and separation. Compos. Commun2018, 8, 92–100.
11. Garcia-Galan C; Berenguer-Murcia Á; Fernandez-Lafuente R; Rodrigues RC, Potential of different enzyme immobilization strategies to improve enzyme performance. Adv. Synth. Catal2011, 353 (16), 2885–2904.
12. Taniguchi M; Kobayashi M; Fujii M, Properties of a reversible soluble–insoluble cellulase and its application to repeated hydrolysis of crystalline cellulose. Biotechnol. Bioeng1989, 34 (8), 1092–1097. [PubMed: 18588203]
13. Cannell DS; Rondelez F, Diffusion of polystyrenes through microporous membranes. Macromolecules1980, 13 (6), 1599–1602.
14. Davidson MG; Deen WM, Hindered diffusion of water-soluble macromolecules in membranes. Macromolecules1988, 21 (12), 3474–3481.
15. Deen W, Hindered transport of large molecules in liquid-filled pores. AlChE J. 1987, 33 (9), 1409–1425.
16. Yao Y; Lenhoff AM, Pore size distributions of ion exchangers and relation to protein binding capacity. J. Chromatogr. A2006, 1126 (1–2), 107–119. [PubMed: 16844131]
17. Lustig SR; Peppas NA, Solute diffusion in swollen membranes. IX. Scaling laws for solute diffusion in gels. J. Appl. Polym. Sci1988, 36 (4), 735–747.
18. Liu D; Kotsmar C; Nguyen F; Sells T; Taylor N; Prausnitz J; Radke C, Macromolecule sorption and diffusion in HEMA/MAA hydrogels. Ind. Eng. Chem2013, 52 (50), 18109–18120.
19. Vagias A; Sergelen K; Koynov K; Kosovan P; Dostalek J; Jonas U; Knoll W; Fytas G, Diffusion and Permeation of Labeled IgG in Grafted Hydrogels. Macromolecules2017, 50 (12), 4770–4779.
20. Clague DS; Phillips RJ, Hindered diffusion of spherical macromolecules through dilute fibrous media. Phys. Fluids1996, 8 (7), 1720–1731.
21. Punyaratabandhu N; Kongoup P; Dechadilok P; Katavetin P; Triampo W, Transport of Spherical Particles Through Fibrous Media and a Row of Parallel Cylinders: Applications to Glomerular Filtration. J. Biomech. Eng2017, 139 (12), 121005.
22. Vermonden T; Censi R; Hennink WE, Hydrogels for protein delivery. Chem. Rev2012, 112 (5), 2853–2888. [PubMed: 22360637]
23. Masaro L; Zhu X, Physical models of diffusion for polymer solutions, gels and solids. Prog. Polym. Sci1999, 24 (5), 731–775.
24. Dechadilok P; Deen WM, Hindrance factors for diffusion and convection in pores. Ind. Eng. Chem. Res2006, 45 (21), 6953–6959.
25. Gutenwik J; Nilsson B; Axelsson A, Determination of protein diffusion coefficients in agarose gel with a diffusion cell. Biochem. Eng. J2004, 19 (1), 1–7.

26. Bagherzadeh R; Latifi M; Najar SS; Tehran MA; Kong L, Three-dimensional pore structure analysis of Nano/Microfibrous scaffolds using confocal laser scanning microscopy. J. Biomed. Mater. Res., Part A2013, 101 (3), 765–774.
27. Bagherzadeh R; Latifi M; Kong L, Three-dimensional pore structure analysis of polycaprolactone nano-microfibrous scaffolds using theoretical and experimental approaches. J. Biomed. Mater. Res., Part A2014, 102 (3), 903–910.
28. Amin A; Merati AA; Bahrami SH; Bagherzadeh R, Effects of porosity gradient of multilayered electrospun nanofibre mats on air filtration efficiency. J. Text. Inst2017, 108 (9), 1563–1571.
29. Chen Z; Du X.-a.; Liu Y; Ju Y; Song S; Dong L, A high-efficiency ultrafiltration nanofibrous membrane with remarkable antifouling and antibacterial ability. J. Mater. Chem. A2018, 6 (31), 15191–15199.
30. Durbin L; Kobayashi R, Diffusion of Krypton-85 in Dense Gases. J. Chem. Phys1962, 37 (8), 1643–1654.
31. Fanous J; Swed A; Joubran S; Hurevich M; Britan-Rosich E; Kotler M; Gilon C; Hoffman A, Superiority of the S, S conformation in diverse pharmacological processes: Intestinal transport and entry inhibition activity of novel anti-HIV drug lead. Int. J. Pharm2015, 495 (2), 660–663. [PubMed: 26392249]
32. Stringer JL; Peppas NA, Diffusion of small molecular weight drugs in radiation-crosslinked poly (ethylene oxide) hydrogels. J. Control. Release1996, 42 (2), 195–202.
33. Putnam FW; Prealbumin AT-B; Globulin CT-B; al-Antitrypsin B; Ceruloplasmin A; Haptoglobin C; Hemopexin B, 2 Alpha, Beta, Gamma. The plasma proteins: structure, function, and genetic control1975, 1, 57.
34. Boschetti E, Advanced sorbents for preparative protein separation purposes. J. Chromatogr. A1994, 658 (2), 207–236.
35. Farnan D; Frey D; Horvath C, Surface and pore diffusion in macroporous and gel-filled gigaporous stationary phases for protein chromatography. J. Chromatogr. A2002, 959 (1–2), 65–73. [PubMed: 12141562]
36. Beck RE; Schultz JS, Hindered diffusion in microporous membranes with known pore geometry. Science1970, 170 (3964), 1302–1305. [PubMed: 17829429]
37. Yang X; Liu C; Li Y; Marchesoni F; Hänggi P; Zhang H, Hydrodynamic and entropic effects on colloidal diffusion in corrugated channels. Proc. Natl. Acad. Sci2017, 114 (36), 9564–9569. [PubMed: 28831004]
38. Zhou Y; Li J; Zhang Y; Dong D; Zhang E; Ji F; Qin Z; Yang J; Yao F, Establishment of a physical model for solute diffusion in hydrogel: understanding the diffusion of proteins in poly (sulfobetaine methacrylate) hydrogel. J. Phys. Chem. B2017, 121 (4), 800–814. [PubMed: 28060509]
39. Hettiaratchi MH; Schudel A; Rouse T; García AJ; Thomas SN; Guldberg RE; McDevitt TC, A rapid method for determining protein diffusion through hydrogels for regenerative medicine applications. APL Bioeng. 2018, 2 (2), 026110. [PubMed: 31069307]
40. Wu J; Xiao Z; He C; Zhu J; Ma G; Wang G; Zhang H; Xiao J; Chen S, Protein diffusion characteristics in the hydrogels of poly (ethylene glycol) and zwitterionic poly (sulfobetaine methacrylate)(pSBMA). Acta Biomater. 2016, 40, 172–181. [PubMed: 27142255]
41. Kotsmar C; Sells T; Taylor N; Liu DE; Prausnitz J; Radke C, Aqueous solute partitioning and mesh size in HEMA/MAA hydrogels. Macromolecules2012, 45 (22), 9177–9187.
42. Liu D; Dursch T; Taylor N; Chan S; Bregante D; Radke C, Diffusion of water-soluble sorptive drugs in HEMA/MAA hydrogels. J. Control. Release2016, 239, 242–248. [PubMed: 27565214]
43. Wang L; Fu Q; Yu J; Liu L; Ding B, Nanoparticle-doped polystyrene/polyacrylonitrile nanofiber membrane with hierarchical structure as promising protein hydrophobic interaction chromatography media. Compos. Commun2019, 16, 33–40.
44. Putnam FW, Alpha, beta, gamma, omega—the roster of the plasma proteins. In The plasma proteins, Elsevier: 1975; pp 57–131.
45. Dursch TJ; Taylor NO; Liu DE; Wu RY; Prausnitz JM; Radke CJ, Water-soluble drug partitioning and adsorption in HEMA/MAA hydrogels. Biomaterials2014, 35 (2), 620–629. [PubMed: 24148241]

46. Shin K; Yu H; Kim J, Determination of diffusion coefficient and partition coefficient of photoinitiator 2-hydroxy-2-methylpropiophenone in nanoporous polydimethylsiloxane network and aqueous poly (ethylene glycol) diacrylate solution. J. Ind. Eng. Chem2017, 56, 443–449.
47. Silva D; Azevedo A; Fernandes P; Chu V; Conde J; Aires-Barros M, Determination of partition coefficients of biomolecules in a microfluidic aqueous two phase system platform using fluorescence microscopy. J. Chromatogr. A2017, 1487, 242–247. [PubMed: 28110948]
48. Ogston A, The spaces in a uniform random suspension of fibres. Trans. Faraday Soc1958, 54, 1754–1757.
49. Lazzara MJ; Blankschtein D; Deen WM, Effects of multisolute steric interactions on membrane partition coefficients. J. Colloid Interf. Sci2000, 226 (1), 112–122.
50. Pappenheimer J; Renkin E; Borrero L, Filtration, diffusion and molecular sieving through peripheral capillary membranes: a contribution to the pore theory of capillary permeability. Am. J. Physiol1951, 167 (1), 13–46. [PubMed: 14885465]
51. Bagherzadeh R; Najar SS; Latifi M; Tehran MA; Kong L, A theoretical analysis and prediction of pore size and pore size distribution in electrospun multilayer nanofibrous materials. J. Biomed. Mater. Res., Part A2013, 101 (7), 2107–2117.
52. Khoshui SK; Ravandi SAH; Bagherzadeh R; Saberi Z; Karimi M, Investigation of the pore geometrical structure of nanofibrous membranes using statistical modelling. Appl. Phys. A2016, 122 (10), 1–9.
53. Ahmad A; Low S; Shukor SA; Fernando W; Ismail A, Hindered diffusion in lateral flow nitrocellulose membrane: Experimental and modeling studies. J. Membr. Sci2010, 357 (1–2), 178–184.
54. Phillips R; Deen W; Brady J, Hindered transport of spherical macromolecules in fibrous membranes and gels. AlChE J. 1989, 35 (11), 1761–1769.
55. Johansson L; Elvingson C; Loefroth JE, Diffusion and interaction in gels and solutions. 3. Theoretical results on the obstruction effect. Macromolecules1991, 24 (22), 6024–6029.
56. Johnson EM; Berk DA; Jain RK; Deen WM, Hindered diffusion in agarose gels: test of effective medium model. Biophys. J1996, 70 (2), 1017–1023. [PubMed: 8789119]
57. Renkin EM, Filtration, diffusion, and molecular sieving through porous cellulose membranes. J. Gen. Physiol1954, 38 (2), 225. [PubMed: 13211998]
58. Pappenheimer JR, Passage of molecules through capillary walls. Physiol. Rev1953, 33 (3), 387–423. [PubMed: 13088295]
59. Schmitz KS; Lu M, Effect of titration charge on the diffusion of bovine serum albumin. Proc. Natl. Acad. Sci1983, 80 (2), 425–429. [PubMed: 6572899]
60. Ge S; Kojio K; Takahara A; Kajiyama T, Bovine serum albumin adsorption onto immobilized organotrichlorosilane surface: influence of the phase separation on protein adsorption patterns. J. Biomater. Sci., Polym. Ed1998, 9 (2), 131–150. [PubMed: 9493841]
61. Axelsson I, Characterization of proteins and other macromolecules by agarose gel chromatography. J. Chromatogr. A1978, 152 (1), 21–32.
62. Wetter L; Deutsch H, Immunological studies on egg white proteins. J. Biol. Chem1951, 192, 237–242. [PubMed: 14917670]
63. Parmar AS; Muschol M, Hydration and hydrodynamic interactions of lysozyme: effects of chaotropic versus kosmotropic ions. Biophys. J2009, 97 (2), 590–598. [PubMed: 19619474]
64. Brune D; Kim S, Predicting protein diffusion coefficients. Proc. Natl. Acad. Sci1993, 90 (9), 3835–3839. [PubMed: 8483901]
65. Chiodi F; Sidén Å; Ösby E, Isoelectric focusing of monoclonal immunoglobulin G, A and M followed by detection with the avidin-biotin system. Electrophoresis1985, 6 (3), 124–128.
66. Saltzman WM; Radomsky ML; Whaley KJ; Cone RA, Antibody diffusion in human cervical mucus. Biophys. J1994, 66 (2), 508–515. [PubMed: 8161703]
67. Lavery CB; MacInnis MC; MacDonald MJ; Williams JB; Spencer CA; Burke AA; Irwin DJ; D'Cunha GB, Purification of peroxidase from horseradish (Armoracia rusticana) roots. J. Agric. Food. Chem2010, 58 (15), 8471–8476. [PubMed: 20681636]

68. Engberg K; Frank CW, Protein diffusion in photopolymerized poly (ethylene glycol) hydrogel networks. Biomed. Mater2011, 6 (5), 055006. [PubMed: 21873762]

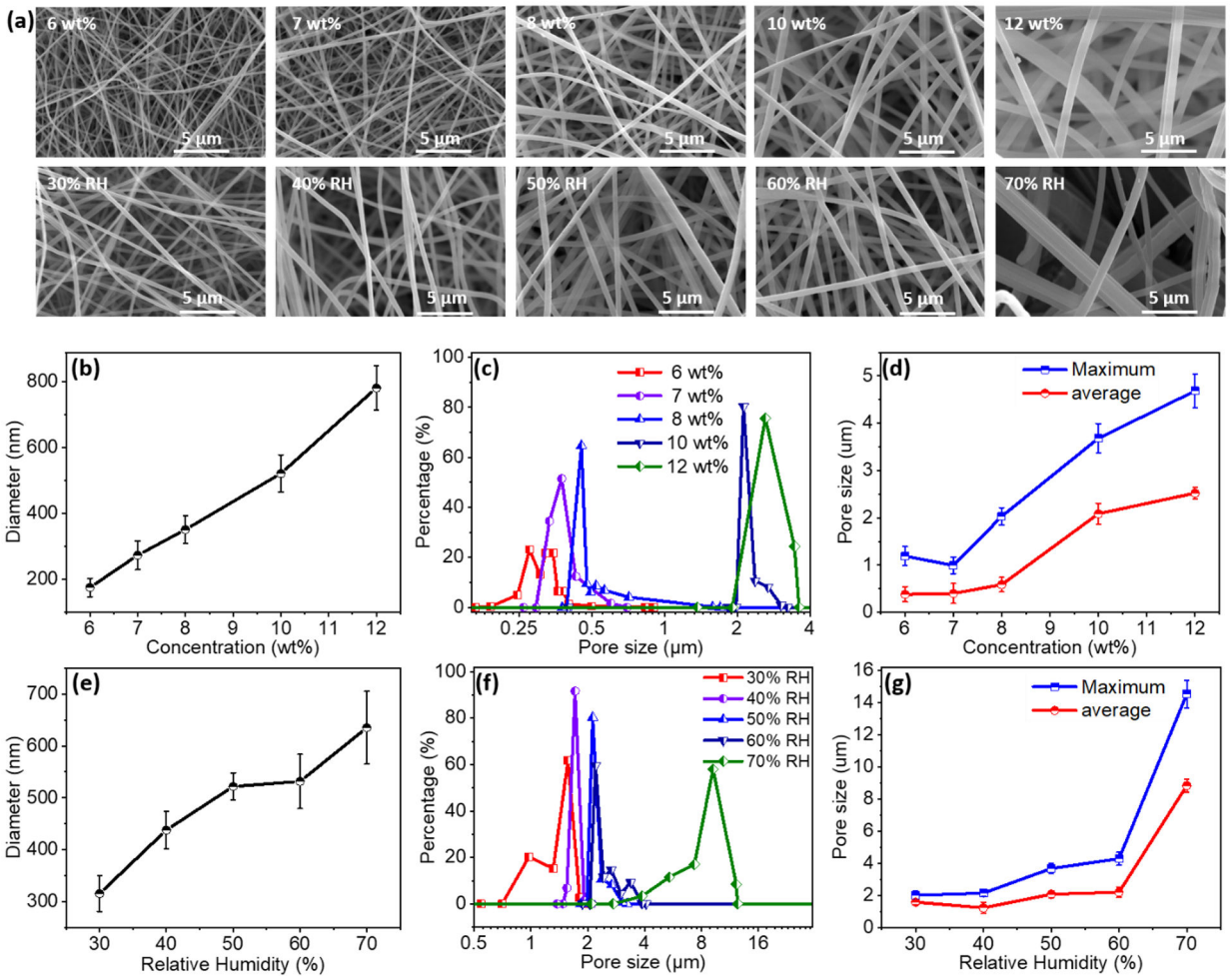

Figure 1.

(a) SEM images of PAN nanofibrous membranes made under different polymer concentrations and relative humidity; and fiber diameters, pore distributions, pore sizes of as-prepared membranes: (b) and (e) fiber diameter, (c) and (f) measured pore distribution, and (d) and (g) measured maximum pore size and average pore size.

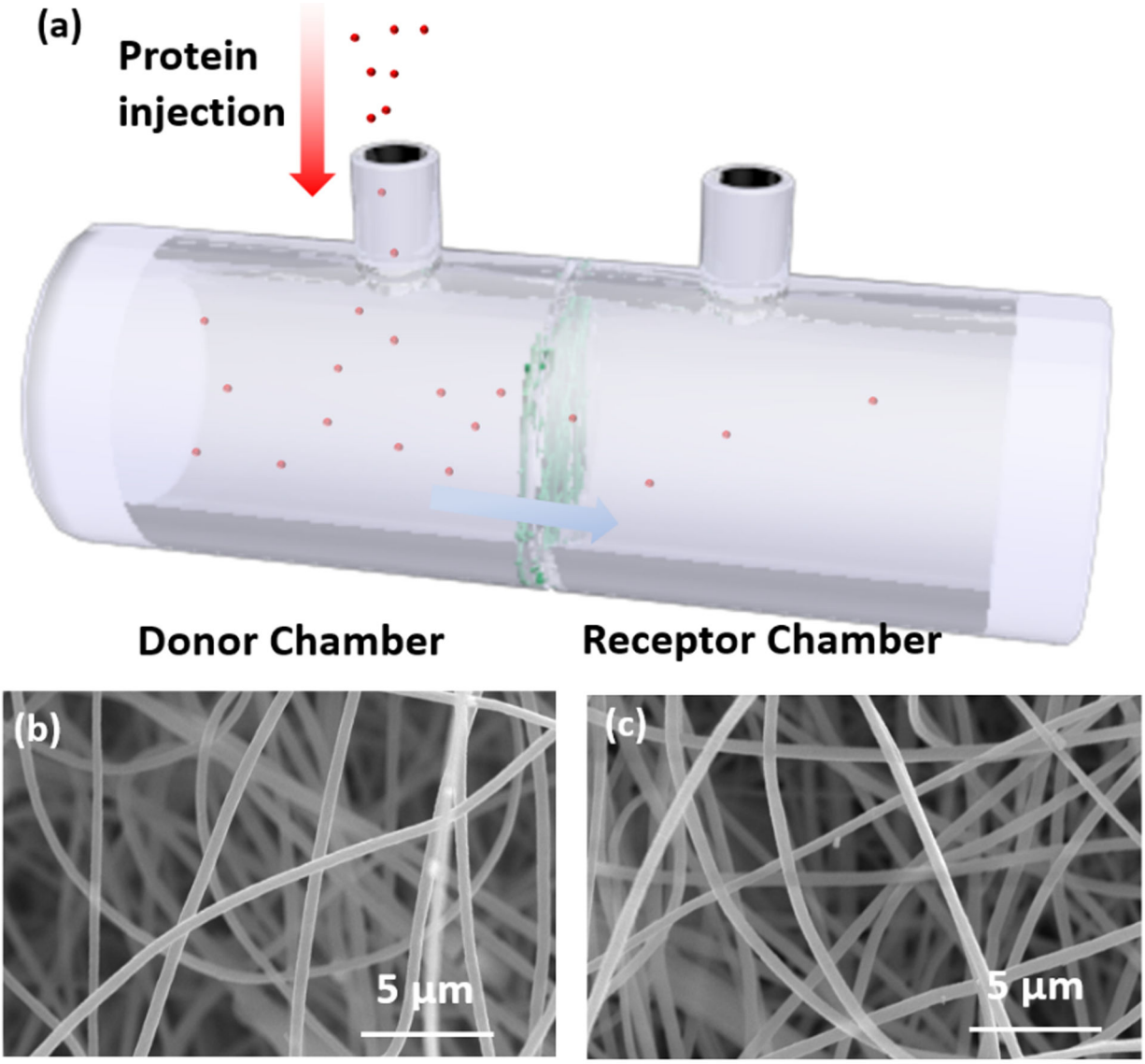

Figure 2.
(a) A scheme of a side-by-side chamber used in this study; (b-c) SEM images of the membrane before and after the diffusion test.

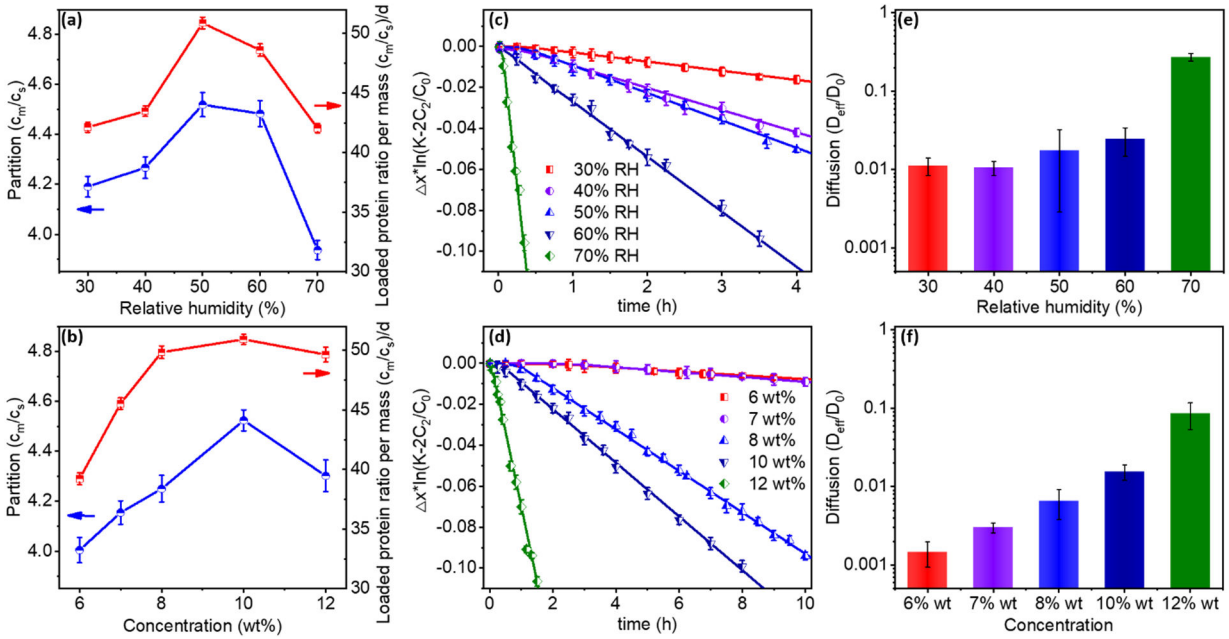

Figure 3.

Partition coefficient of proteins inside membranes prepared (a) under different relative humidity conditions and (b) with different polymer concentrations; cumulative amounts of protein in receptor chamber versus time: (c) PAN membranes prepared under different relative humidity (RH) conditions, (d) membranes prepared with different polymer concentrations; and effective diffusion coefficients of membranes prepared (e) under different relative humidity conditions and (f) with different polymer concentrations.

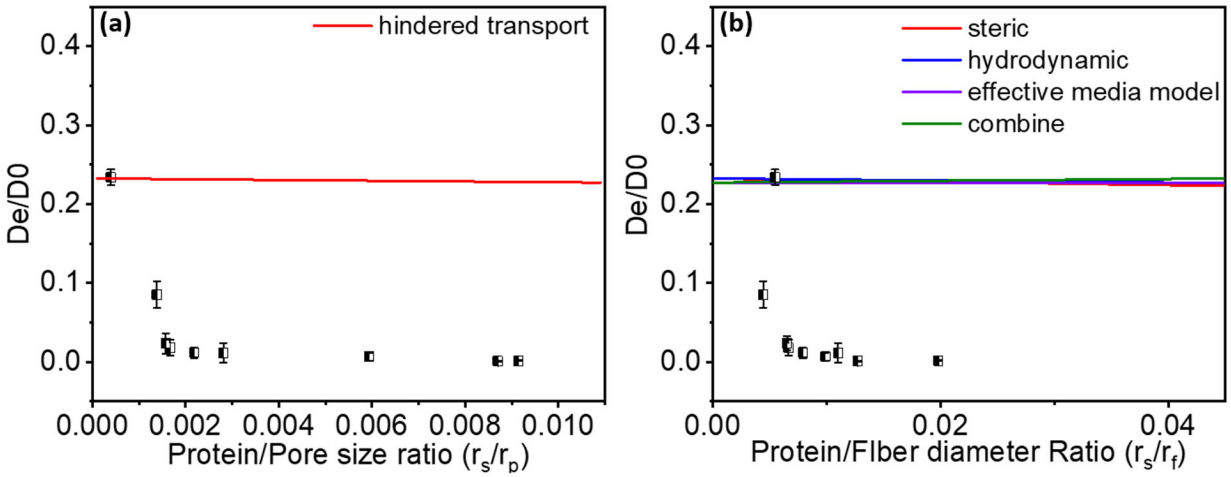

Figure 4.

Measured and predicted results of effective diffusion coefficient ratios of proteins in membranes with different a) protein to measured pore size ratios, and b) protein to fiber diameter ratios

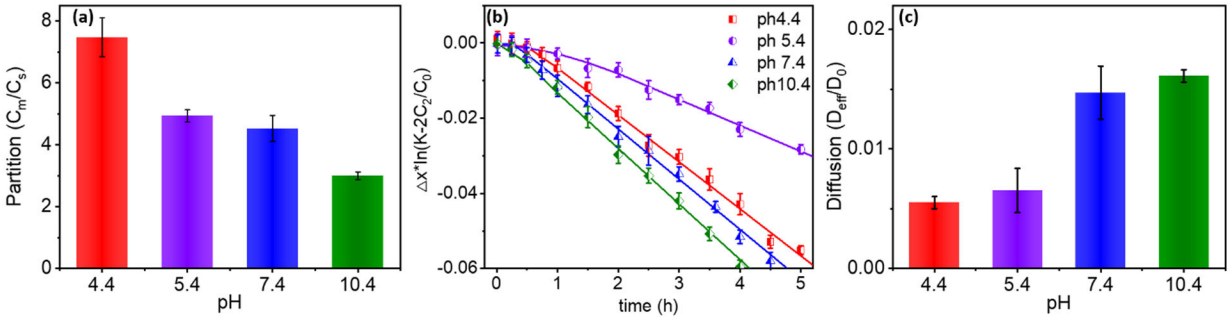

Figure 5.

The impact of pH value on (a) partition coefficient, (b) cumulative amount of BSA in the receptor chamber versus time, and (c) diffusion coefficient of BSA in same PAN nanofibrous membrane

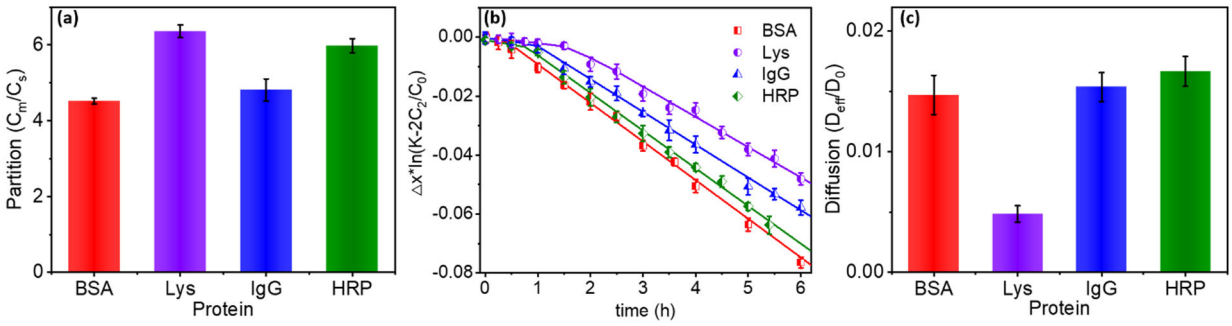

Figure 6.

(a) Partition coefficient of proteins and (b) cumulative amount of protein in the receptor chamber versus time, and (c) diffusion coefficient of four proteins in the same PAN nanofibrous membrane

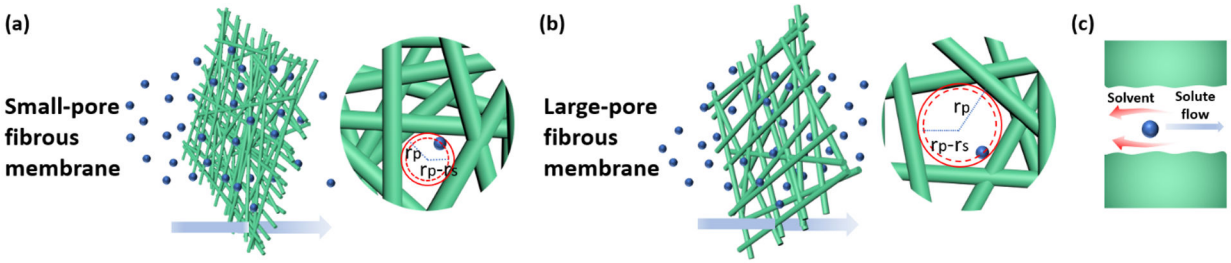

Scheme 1.

The dynamic transport of proteins in small-pore (a) and large-pore (b) fibrous membranes; (c) diffusion of protein through a pore. Where r_p is the average measured pore size, and r_s is a radius of a spherical protein molecule.

Table 1.

The classical diffusion models of molecular through fibrous media

Model type	expression[a]	ref
steric	$\frac{D}{D_0} = \exp(-\sqrt{\sigma})$	Ogston et al.[48]
hydrodynamic	$\frac{D}{D_0} = \left[1 + \left(\frac{r_s^2}{k}\right)^{\frac{1}{2}} + \frac{1}{3}\frac{r_s^2}{k}\right]^{-1}$	Phillips et al.[54]
effective media model	$\frac{D}{D_0} = \exp[-0.84\varphi(\sigma)]^{1.09}$	Johansson et al.[55]
combined	$\frac{D}{D_0} = \frac{\exp[-0.84\varphi(\sigma)]^{1.09}}{\left[1 + \left(\frac{r_s^2}{k}\right)^{\frac{1}{2}} + \frac{1}{3}\frac{r_s^2}{k}\right]}$	Johnson et al.[56]
hindered transport	$\frac{D}{D_0} = (1 - \frac{r_s}{r_p})^2\left[1 - 2.10\frac{r_s}{r_p} + 2.09(\frac{r_s}{r_p})^3 - 0.95\left(\frac{r_s}{r_p}\right)^5\right]$	Renkin.[57] Pappenheimer et al.[58]

[a]: $\sigma = \varphi\left(1 + \frac{r_s}{r_f}\right)^2$;

$k = 0.31 r_f^2 \varphi^{-1.17}$

Table 2

Parameters of four different proteins: BSA, Lysozyme, IgG and HRP

Protein	pI	r_s (nm)	D_0 (cm^2/s)
BSA	5.4[60]	3.48[61]	$5.9*10^{-7}$ [33]
Lysozyme	11.35[62]	1.85[63]	$1.11\pm0.05*10^{-6}$ [64]
IgG	6.6 – 7.2[65]	5.4[66]	$4.4\pm1.3*10^{-7}$ [66]
HRP	8.8[67]	3.0[68]	$7.57*10^{-7}$ [68]